RSC Advances

PAPER

View Article Online
View Journal | View Issue

Published on 29 August 2016. Downloaded by Synchrotron Radiation Library on 11/09/2017 04:24:32.

Cite this: *RSC Adv.*, 2016, **6**, 83448

Benzothiophene-flanked diketopyrrolopyrrole polymers: impact of isomeric frameworks on carrier mobilities†

Jianyao Huang,‡[a] Xiaotong Liu,‡[ab] Dong Gao,[ab] Congyuan Wei,[ab] Weifeng Zhang[a] and Gui Yu*[ab]

Received 21st July 2016
Accepted 29th August 2016

DOI: 10.1039/c6ra18573h

www.rsc.org/advances

Exploring new building blocks for solution-processable polymeric semiconductors has attracted much attention. We herein develop two isomeric benzothiophene-flanked diketopyrrolopyrrole polymers with different linkage positions and further systematically study the electronic structures, optical properties, and field-effect characteristics. Both polymers exhibit typical p-type transport characteristics with the highest mobility being up to 0.80 $cm^2 V^{-1} s^{-1}$. Our results suggest that the isomeric backbones for conjugated polymers greatly affect charge transport properties.

Introduction

Systematic study of polymeric semiconductors utilized for flexible opto-electronic technologies has emerged as a rising research field.[1–16] Different from small molecules, polymeric semiconductors possess more unpredictable characteristics that influence effective charge transport, including complex intra- and intermolecular interactions. For semiconductors used in polymeric field-effect transistors (FETs), both experimental results and theoretical suggestions have confirmed that backbone conjugation and coplanarity are essential factors to achieve high charge carrier mobilities. A high extent of conjugation guarantees the appropriate energy levels of frontier molecular orbitals, and a highly planar backbone ensures good π-orbital overlap and leads to tight packing. However, excessive rigidity of backbone might also make molecules less soluble and not viable for solution processing techniques. One should strike a balance between these interrelated factors when designing new semiconductors.

On the basis of previous works, a successful strategy to obtain high-performance polymer semiconductors is the alternating donor–acceptor (D–A) architecture.[17–22] D–A polymers not only provide tunable frontier molecular orbital energy levels to ensure the effective charge carrier injection at the semiconductor/electrode interface, but also bring about intramolecular interactions to promote backbone ordering.[23] In addition, the introduction of electron-withdrawing moieties can deplete π-electron density of the main chain, relieving the electrostatic repulsion and enhancing stacking interactions between neighbouring strands.[24] Diketopyrrolopyrrole (DPP) has been receiving considerable attention for constructing D–A polymers for organic field-effect transistors with mobilities greater than 1 $cm^2 V^{-1} s^{-1}$. The electron-deficient nature of DPP moieties was thought efficient for low band gap materials.[25,26] As a lactam building block, side chains could be readily introduced to enhance the solubility and self-assembly and to further control the interdigitation and crystallinity.[4,27,28] Intramolecular hydrogen bonds also occur as a conformational lock between the carbonyl group and adjacent substituents in DPP moiety, allowing the perfect coplanar polymer backbone. Thiophene-flanked DPP has been the most widely investigated building block. The replacement of the flanking thiophene with more conjugated units, *e.g.* thienothiophene (Fig. 1), tends to

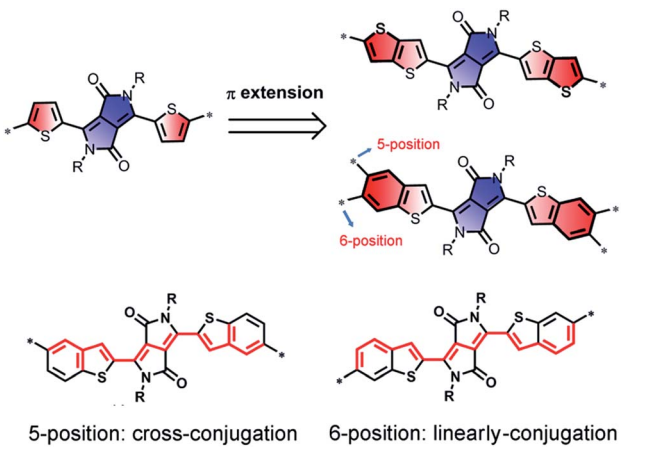

Fig. 1 Structures of benzothiophene-flanked DPP and related analogues.

[a]*Beijing National Laboratory for Molecular Sciences, Institute of Chemistry, Chinese Academy of Sciences, Beijing 100190, P. R. China. E-mail: yugui@iccas.ac.cn*

[b]*University of Chinese Academy of Sciences, Beijing 100049, P. R. China*

† Electronic supplementary information (ESI) available. See DOI: 10.1039/c6ra18573h

‡ These authors contributed equally to this work.

This journal is © The Royal Society of Chemistry 2016

Published on 29 August 2016. Downloaded by Synchrotron Radiation Library on 11/09/2017 04:24:32.

promote a more delocalized frontier orbital distribution and enhance intermolecular interactions.[29,30] Benzothiophene fragment is also a conventional building block for high-performance organic semiconductors.[31–33] Considering the possible C–H$\cdots\pi$, π–π and S$\cdots$S interactions brought by this conjugated moiety that may facilitate charge transport, we herein synthesized benzothiophene-flanked DPP monomer to investigate its properties and applications in OFETs.

To probe into the intrinsic structure–property–device performance correlations, it is of particular interest to synthesize small molecule or polymeric semiconductors with isomeric structures.[34–42] Among these molecules, cross-conjugated semiconductors are relatively unexplored. The distinct electronic structures of these semiconducting materials can exert significant influence over optical and electrochemical properties,[34] and consequently have an impact on charge transport. Benzothiophene-containing systems provide several linkage positions in which cross conjugation may derive solely from a particular substitution pattern.[34] To design polymeric semiconductors utilized for FETs, backbone linearity is supposed to be an initial factor for sufficient π-stacks. For the benzothiophene subunit, two substitution positions are possible in terms of obtaining a relatively linear backbone. We herein prepared both 5- and 6-bonded polymers to systematically study the charge transport properties. Different linkage positions lead to linearly- or cross-conjugated polymers, *i.e.* 5-bonded polymer exhibits a cross-conjugated electronic structure whereas the 6-bonded analogue is linearly conjugated (Fig. 1). In this work, 1,2-dithienylethene comonomer was introduced to obtain analogous poly[dibenzothiophenyl diketopyrrolopyrrole-*alt*-dithienylethene] (PBTDPP-DTE). Properties, characterisation, and PFET performance of both polymers are reported. Because of the conjugation diversity of electronic structures, we provide a further insight into the influence of linear-to-cross conjugation changes in field-effect characteristics. Additionally, cross-conjugated polymers result in strong aggregate tendencies and exhibit shorter spacing between main chains than that of the linearly-conjugated isomer, allowing us to investigate the fundamentals of charge transporting pathways.

Experimental

Instruments and measurement

The reagents and starting materials employed were commercially available and used without any further purification unless otherwise indicated. Anhydrous solvent was purified with a standard distillation procedure prior to use. ^{1}H NMR and ^{13}C NMR spectra were recorded on a Bruker DMX 300 spectrometer. Chemical shifts are reported as δ values [ppm] relative to internal tetramethylsilane (TMS). Electron-impact (EI) mass spectra were collected on a GCI-MS micromass (UK) spectrometer. MALDI-TOF mass spectra were collected on an Autoflex III (Bruker Daltonics Inc.) MALDI-TOF spectrometer. UV-vis-NIR absorption spectra were recorded on a Jasco-570 spectrophotometer. Cyclic voltammetric measurements were carried out on a CHI660c electrochemical workstation. Molecular weights were determined with gel permeation chromatography (GPC) at 150 °C on a PL-220 system using 1,2,4-trichlorobenzene as the eluent.

Materials and synthesis

PFETs were fabricated on highly-doped silicon wafer with 300 nm silicon oxide insulator. The source-drain gold electrodes were prepared using photolithography. The substrates were then subjected to cleaning using ultrasonication in acetone, deionized water (twice), and ethanol. The cleaned substrates were dried in vacuum at 80 °C and treated with UVO for 20 min. Before the deposition of polymer semiconductors, octadecyltrichlorosilane (OTS) treatment was performed on the silicon oxide gate dielectrics in vacuum to form a self-assembled OTS monolayer. Then, a layer of polymer semiconductor film was spin-coated on the OTS-treated substrates from a polymer solution in hot *o*-dichlorobenzene or chloroform at an optimized speed. For annealing FETs, the samples were further placed on a hotplate in air for 5 min at an optimized temperature (see ESI†) before being allowed to cool to room temperature. Field-effect characteristics of the devices were determined in air by using a Keithley 4200 SCS semiconductor parameter analyzer. The field-effect mobility in saturation (μ) is calculated from equation: $I_{DS} = (W/2L)C_i\mu(V_{GS} - V_{th})^2$, where W/L is the channel width/length, C_i is the gate dielectric layer capacitance per unit area, and V_{GS} and V_{th} are the gate voltage and threshold voltage, respectively.

Ethyl 6-bromobenzo[*b*]thiophene-2-carboxylate (1a). To a solution of 4-bromo-2-fluorobenzaldehyde (25.00 g, 123.2 mmol) in anhydrous dimethylformamide (DMF, 120 mL) was added K_2CO_3 (22.08 g, 160 mmol) under an ice bath. The reaction mixture was stirred for 0.5 h before addition of ethyl 2-mercaptoacetate (13.6 mL, 1.05 eq.) dropwise. The mixture was warmed up to room temperature and stirred overnight. The reaction mixture was then heated to 55 °C and stirred under this temperature for 5 h. The resultant mixture was cooled and water (300 mL) was added. The precipitate was filtered, washed with ethanol to afford a white solid (32.3 g, yield: 92%). EI-MS *m*/*z*: 284 (^{79}Br), 286 (^{81}Br); ^{1}H NMR (300 MHz, $CDCl_3$) δ (ppm): 7.957 (s, 2H), 7.674 (d, 1H, J = 8.7 Hz), 7.481–7.448 (m, 1H), 4.397 (q, 2H, J = 7.2 Hz), 1.405 (t, 3H, J = 7.2 Hz); ^{13}C NMR (75 MHz, $CDCl_3$) δ (ppm): 162.39, 143.43, 137.38, 134.47, 129.82, 128.51, 126.49, 125.24, 121.16, 61.77, 14.33.

Ethyl 5-bromobenzo[*b*]thiophene-2-carboxylate (1b). The procedure was similar to **1a** by replacement of the starting material with 5-bromo-2-fluorobenzaldehyde. Yield: 85%. EI-MS *m*/*z*: 284 (^{79}Br), 286 (^{81}Br); ^{1}H NMR (300 MHz, $CDCl_3$) δ (ppm): 7.973 (d, 1H, J = 1.8 Hz), 7.931 (s, 1H), 7.688 (d, 1H, J = 8.4 Hz), 7.507 (dd, 1H, J_1 = 8.4 Hz, J_2 = 1.8 Hz), 4.406 (q, 2H, J = 7.2 Hz), 1.412 (t, 3H, J = 7.2 Hz); ^{13}C NMR (75 MHz, $CDCl_3$) δ (ppm): 162.33, 140.61, 140.21, 135.69, 129.92, 129.19, 127.90, 124.09, 118.87, 61.82, 14.33.

6-Bromobenzo[*b*]thiophene-2-carbonitrile (2a). To a solution of $LiAlH_4$ (2.885 g, 76 mmol) in tetrahydrofuran (THF, 60 mL) was added **1a** (11.4 g, 40 mmol) in anhydrous THF (60 mL) dropwise under an ice bath. The resulting mixture was stirred for 1 h before being quenched with water. The mixture was

Published on 29 August 2016. Downloaded by Synchrotron Radiation Library on 11/09/2017 04:24:32.

extracted with ethyl acetate and dried over with Na_2SO_4 to afford a white solid as the corresponding alcohol. The residue was dissolved in dichloromethane, transferred to a suspension of pyridinium chlorochromate (PCC)/silica gel (m m^{-1} 1 : 1, PCC 1.5 eq.) in CH_2Cl_2 and stirred for 3 h until the starting material was consumed. The solvent was evaporated, and the residue was diluted with ether and passed a panel of 5 cm silica gel to afford an orange solid as the aldehyde. The solid was then dissolved in THF. 2 eq. I_2 and 10 mL $mmol^{-1}$ 28% ammonia was added in batches. The solution was stirred overnight at room temperature, extracted with ethyl acetate, washed with saturated $Na_2S_2O_3$ solution, and dried over $MgSO_4$. Purification by column chromatography on silica gel with ethyl acetate/light petroleum (1 : 4) as the eluent yielded 8.2 g as a white solid. Yield: 86%. ^{1}H NMR (300 MHz, $CDCl_3$) δ (ppm): 8.002 (m, 1H), 7.838 (s, 1H), 7.736 (d, 1H, J = 8.7 Hz), 7.587–7.553 (m, 1H); ^{13}C NMR (75 MHz, $CDCl_3$) δ (ppm): 142.52, 136.16, 134.61, 129.52, 126.26, 124.96, 122.47, 113.98, 110.27. HR EI-MS m/z (M^+): calcd for C_9H_4BrNS, 236.9248; found, 236.9250.

5-Bromobenzo[*b*]thiophene-2-carbonitrile (2b). The procedure was similar to **2a** by replacement of the starting material with ethyl **1b**. The target product is a white solid. Yield: 83%. ^{1}H NMR (300 MHz, $CDCl_3$) δ (ppm): 8.032 (d, 1H, J = 1.8 Hz), 7.812 (s, 1H), 7.726 (d, 1H, J = 8.7 Hz), 7.618 (dd, 1H, J_1 = 8.7 Hz, J_2 = 1.8 Hz); ^{13}C NMR (75 MHz, $CDCl_3$) δ (ppm): 139.75, 138.96, 133.88, 131.06, 127.78, 123.70, 119.94, 113.87, 111.54. HR EI-MS m/z (M^+): calcd for C_9H_4BrNS, 236.9248; found, 236.9251.

3,6-Bis(6-bromobenzo[*b*]thiophen-2-yl)pyrrolo[3,4-*c*]pyrrole-1,4(2*H*,5*H*)-dione (3a). To a solution of $NaO^tC_5H_{11}$ (5.69 g, 51.6 mmol) in *tert*-amyl alcohol (40 mL) was added **2a** (8.2 g, 34.44 mmol) under argon atmosphere at 85 °C. The mixture was stirred for 5 min before addition of diisopropyl succinate (2.79 g, 13.78 mmol) dropwise. The reaction mixture was stirred at this temperature for 2 h, then cooled down to 50 °C, diluted with methanol (30 mL), and neutralized with AcOH (*ca.* 10 mL). The mixture was cooled to room temperature, filtered and the resulting residue was washed with water, hot methanol, acetone and hexane to yield a purple solid (6.1 g, yield: 79%). This compound was used in the next step without further purification.

3,6-Bis(5-bromobenzo[*b*]thiophen-2-yl)pyrrolo[3,4-*c*]pyrrole-1,4(2*H*,5*H*)-dione (3b). The procedure was similar to **3a** by replacement of the starting material with **2b**. This compound was used in the next step without further purification.

3,6-Bis(6-bromobenzo[*b*]thiophen-2-yl)-2,5-bis(2-decyltetradecyl)pyrrolo[3,4-*c*]pyrrole-1,4(2*H*,5*H*)-dione (6BrBTDPP). To a solution of **3a** (3.0 g, 5.37 mmol) in DMF (30 mL) were added potassium carbonate (3.0 g, 21.7 mmol) and 18-crown-6 (~20 mg). The suspension was stirred at 100 °C for 1 h before addition of 2-decyl-1-tetradecyl iodide (7.60 g, 16.36 mmol). The mixture was heated with stirring at 120 °C for 24 h and subsequently cooled to room temperature. Solvent was evaporated to afford the crude product which was sonicated in methanol, ethanol/hexane and further purified by column chromatography (10 : 1–3 : 1, petroleum ether : dichloromethane) on silica gel to afford the title compound as a purple solid (2.31 g, 35%). ^{1}H NMR (300 MHz, $CDCl_3$) δ (ppm): 9.047 (s, 2H), 7.946 (s, 2H), 7.728 (d, 2H, J = 8.7 Hz), 7.476 (dd, 2H, J_1 = 8.7 Hz, J_2 = 1.8 Hz), 4.039 (d, 4H, J = 7.8 Hz), 1.885 (m, 2H), 1.18–1.29 (m, 80H), 0.893–0.833 (m, 12H); ^{13}C NMR (75 MHz, $CDCl_3$) δ (ppm): 161.49, 142.60, 140.74, 137.45, 131.96, 129.47, 128.86, 126.25, 124.47, 121.07, 109.70, 46.45, 37.94, 31.94, 31.22, 30.03, 29.68, 29.59, 29.38, 26.24, 22.70, 14.13. HR MALDI-TOF calcd for $C_{70}H_{106}Br_2N_2O_2S_2$: 1230.6042, found: 1230.6033.

3,6-Bis(5-bromobenzo[*b*]thiophen-2-yl)-2,5-bis(2-decyltetradecyl)pyrrolo[3,4-*c*]pyrrole-1,4(2*H*,5*H*)-dione (5BrBTDPP). The procedure was similar to **6BrBTDPP** by replacement of the starting material with **3b** to afford a dark purple solid with a yield of 33%. ^{1}H NMR (300 MHz, $CDCl_3$) δ (ppm): 8.968 (s, 2H), 8.058 (d, 2H, J = 1.8 Hz), 7.702 (d, 2H, J = 8.7 Hz), 7.510 (dd, 2H, J_1 = 8.7 Hz, J_2 = 1.8 Hz), 4.052 (d, 4H, J = 7.5 Hz), 1.888 (m, 2H), 1.18–1.29 (m, 80H), 0.892–0.835 (m, 12H); ^{13}C NMR (75 MHz, $CDCl_3$) δ (ppm): 161.26, 140.67, 140.06, 139.72, 131.02, 130.56, 129.74, 127.50, 123.06, 119.21, 109.67, 46.37, 37.83, 31.94, 31.25, 30.03, 29.69, 29.60, 29.39, 26.24, 22.70, 14.13. HR MALDI-TOF calcd for $C_{70}H_{106}Br_2N_2O_2S_2$: 1230.6042, found: 1230.6038.

General procedures for polymerization

To a 25 mL Schlenk tube were added thiophenyl ethene stannane (1 eq.), dibromobenzothiophene DPP (1 eq.), a certain amount of $Pd_2(dba)_3$ (dba = dibenzylideneacetone), tri(*o*-tolyl) phosphine, and dry toluene. The tube was charged with argon through a freeze–pump–thaw cycle for three times. The mixture was stirred for 24 h at 110 °C under argon atmosphere before being poured into a mixture of 200 mL of methanol and 15 mL of 6 M aq. HCl. The mixture was stirred for 3 h, filtered, and the residue was then further purified by Soxhlet extraction with methanol, acetone, hexane and chloroform to remove the low-molecular-weight fraction and residual catalyst. The residue was finally extracted with chlorobenzene to afford the resulting polymer.

P_6BTDPP-DTE. (*E*)-1,2-Bis(5-(trimethylstannyl)thiophen-2-yl) ethene (103.6 mg, 0.2 mmol), **6BrBTDPP** (246.3 mg, 0.2 mmol), $Pd_2(dba)_3$ (9 mg), P(*o*-tol)$_3$ (24.6 mg) were reacted in toluene (5 mL) for 24 h to afford a dark polymer (229.7 mg, 91%). GPC: M_n = 18.6 kDa, PDI = 2.18. ^{1}H NMR (300 MHz, $CDCl_3$) δ (ppm): 9.19–9.13 (br, 2H), 8.03–7.51 (m, 8H), 7.03–6.84 (m, 4H), 4.10 (br, 4H), 1.98 (br, 2H), 1.32–1.20 (m, 80H), 0.85 (br, 12H).

P_5BTDPP-DTE. (*E*)-1,2-bis(5-(trimethylstannyl)thiophen-2-yl) ethene (103.6 mg, 0.2 mmol), **5BrBTDPP** (246.3 mg, 0.2 mmol), $Pd_2(dba)_3$ (9 mg), P(*o*-tol)$_3$ (24.6 mg) were reacted in toluene (5 mL) for 24 h to afford a dark polymer (234.7 mg, 93%). GPC: M_n = 19.8 kDa, PDI = 2.32. ^{1}H NMR (300 MHz, $CDCl_3$) δ (ppm): 9.16 (br, 2H), 8.21 (br, 2H), 7.86 (m, 2H), 7.70 (m, 2H), 7.45 (m, 2H), 7.07–7.05 (m, 4H), 4.12 (br, 4H), 1.97 (br, 2H), 1.32–1.20 (m, 80H), 0.87 (br, 12H).

Results and discussion

Synthesis

The synthesis of the monomer was conducted using the procedure analogous to those of 3,6-bis(4-bromophenyl)-2,5-dialkylpyrrolo[3,4-*c*]pyrrole-1,4-(2*H*,5*H*)-dione and 3,6-bis(thiophen-2-yl)-2,5-dialkylpyrrolo[3,4-*c*]pyrrole-1,4-(2*H*,5*H*)-dione.

 This journal is © The Royal Society of Chemistry 2016

Published on 29 August 2016. Downloaded by Synchrotron Radiation Library on 11/09/2017 04:24:32.

The synthetic route is outlined in Scheme 1. The key step was to synthesize the corresponding cyano-substituted compounds. A preliminary attempt of direct conversion of carboxylate to carbonitrile according to previously reported procedure gave a low yield,[43] which was probably due to the limited solubility of the intermediate. Our modified approach involved a transformation from carboxylate to carbonitrile *via* a multiple-step procedure. Brominated benzothiophene-2-carboxylate was obtained *via* conventional Fiesselmann thiophene synthesis, followed by reduction, PCC oxidation, and treatment with iodine and ammonia water to successfully afford the corresponding brominated benzothiophene-2-carbonitrile.[44] Both polymers, **P$_5$BTDPP-DTE** and **P$_6$BTDPP-DTE**, were synthesized under standard Stille coupling conditions in the presence of tris(dibenzylideneacetone)dipalladium(0) as the catalyst and tri(*o*-tolyl)phosphine as the ligand. The polymers were purified using Soxhlet extraction with methanol, acetone, hexane, and chloroform to remove low-molecular-weight oligomers and residual catalysts. Gel-permeation chromatography (GPC) measurements were performed at 150 °C to avoid the overestimation of molecular weights arising from the pronounced aggregate tendencies of DPP-based polymers. Moderate number-average molecular weights were obtained (M_n = 19.8 and 18.6 kDa for **P$_5$BTDPP-DTE** and **P$_6$BTDPP-DTE**, respectively) using chlorobenzene as the extraction solvent. Because of the rigidity of polymer backbone, both polymers showed limited solubility in common organic solvents at room temperature. Therefore, the following measurements of FET characteristics were carried out using hot *o*-dichlorobenzene as the solvent. Thermogravimetric analysis and differential scanning calorimetry were characterised to study the thermal stability of these polymers. The decomposition temperatures with 5% weight loss of both polymers were about 320 °C and no obvious glass transition was observed from the DSC characterisation from 30 to 300 °C under nitrogen atmosphere.

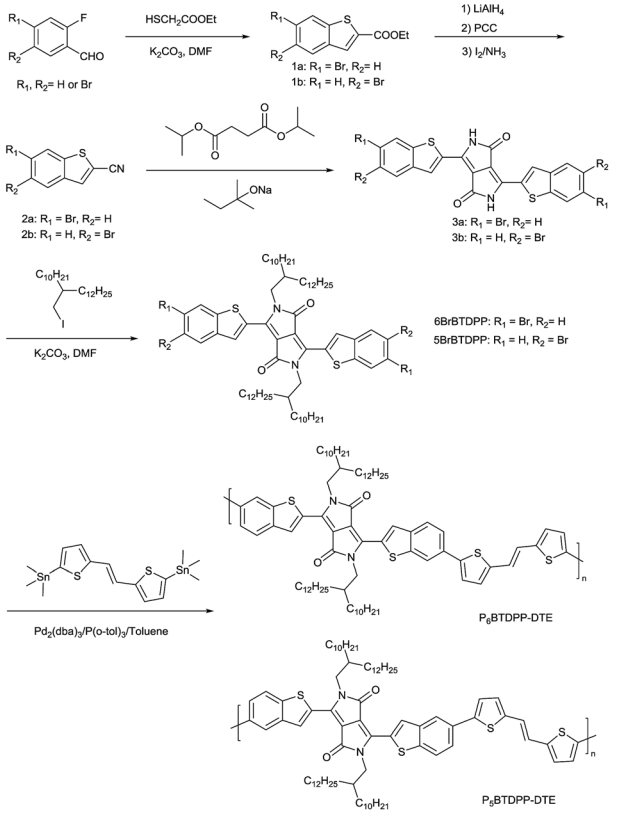

Scheme 1 Synthetic route toward benzothiophene-flanked DPP polymers.

Theoretical studies

The determinant factors affecting optoelectronic properties of organic chromophores are conjugation, aromaticity, planarity, and quinoidal contribution. In this work, both polymers have the identical monomer structures (benzothiophene-flanked DPP and dithienylethene), therefore, the influence of aromaticity should be negligible. The influences of conjugation, planarity, and quinoidal contribution in this work are interrelated. The quinoidal contribution in the linearly-conjugated **P$_6$BTDPP-DTE** plays a much important role than that in the cross-conjugated **P$_5$BTDPP-DTE**, because the cross-conjugation breaks effective π-extension. The intrinsic dihedral angles between benzene-thiophene subunits bring about a nonplanar backbone. The linkage bond between benzene and thiophene subunits has weak double bond character because of the decreased quinoidal mesomeric form.[45] The key influencing factor to the electronic structures of both polymers should be the effective conjugation. We performed theoretical studies to investigate the electronic structure of benzothiophene-flanked DPP. Density functional theory (DFT) calculations of monomer and frontier molecular orbital distributions of trimmers were performed at the B3LYP/6-31G(d) level. As shown in Fig. 2, molecular modeling of benzothiophene-flanked DPP monomer discloses the existence of intramolecular hydrogen-bond (C–H···O, 2.108 Å) between the β-hydrogen of the benzothiophene ring and the carbonyl group, implying the presence of a stable conformation. An approximately planar backbone with torsion angle of *ca.* 0.3° was obtained by calculation. The formation of hydrogen bond is also evident from ^{1}H NMR spectrum, as the signal of β-hydrogen significantly shifts to 8.97–9.05 ppm.[46] The following simulations of trimmers were based on this planar conformation, along with an all trans conformation with respect to adjacent thiophenes to minimize the energies. The side chains were replaced with methyl groups to simplify the calculations. The highest occupied molecular orbital (HOMO) and lowest unoccupied molecular orbital (LUMO) of **P$_6$BTDPP-DTE** are spread out over the entire polymer backbone, setting up an electron density gradient; whereas 5-bonded counterpart displays mainly localized frontier orbitals, indicative of distinct variation of conjugation of these two polymers. Consistent with reported results, dihedral angles between thiophene and benzothiophene planes along the minimum-energy PBTDPP backbones are computed to be 26.8°. The torsion angles are attributed to the C–H···H–C steric hindrance between thiophene and neighbouring benzene segments. On the basis of the theory that high degree of conjugation promotes π-overlaps and

Published on 29 August 2016. Downloaded by Synchrotron Radiation Library on 11/09/2017 04:24:32.

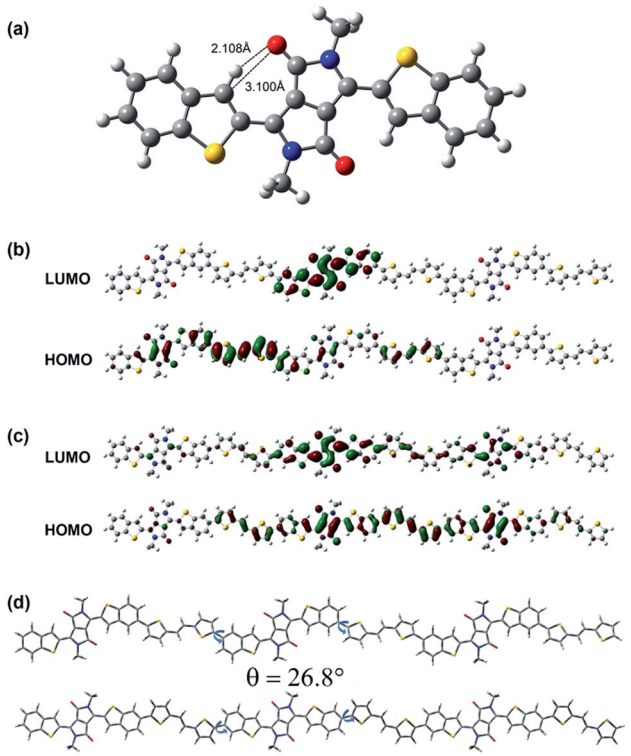

Fig. 2 Possible hydrogen bonding in the energy-minimum conformation (a) and frontier molecular orbital distributions of energy-minimized P_5BTDPP-DTE (b) and P_6BTDPP-DTE (c). (d) Calculated dihedral angles between thiophene and adjacent benzothiophene of both polymers. All calculated using DFT at the B3LYP/6-31G(d) level.

facilitates intramolecular charge transport, a higher mobility of 6-bonded polymer is anticipated.

Optical and electrochemical properties

UV-vis-NIR absorption spectra of the polymers in dilute solution of chlorobenzene and in thin films were carried out to determine the optical properties. As shown in Fig. 3, both **P_5BTDPP-DTE** and **P_6BTDPP-DTE** exhibit typical spectral shapes of D–A polymers. The absorption bands ranging from 300 to 500 nm are assigned to π–π* transition, whereas the absorption maxima at around 600 nm are mainly attributed to intramolecular charge transfer (ICT) character. The 6-bonded **P_6BTDPP-DTE** shows red-shift absorption maxima at 632 and 644 nm in solution and solid state, respectively, compared with the 5-bonded counterpart, suggesting that linear-conjugated polymer exhibits strictly better conjugation than cross-conjugated analogue. Note that 6-bonded **P_6BTDPP-DTE** has a broad ICT band with large oscillator strength, inferring high degree of frontier molecular orbital overlaps. This result is consistent with theoretical modelling. Optical bandgaps of **P_5BTDPP-DTE** and **P_6BTDPP-DTE** were estimated to be 1.60 and 1.56 eV from the onset of absorption, respectively. The relatively small variation in bandgaps was in accordance with previously reported theoretical modelling, in which introducing cross-conjugation greatly affects the oscillator strength but has a negligible effect on the band gap.[41] The differences between absorption spectra of the two polymers are

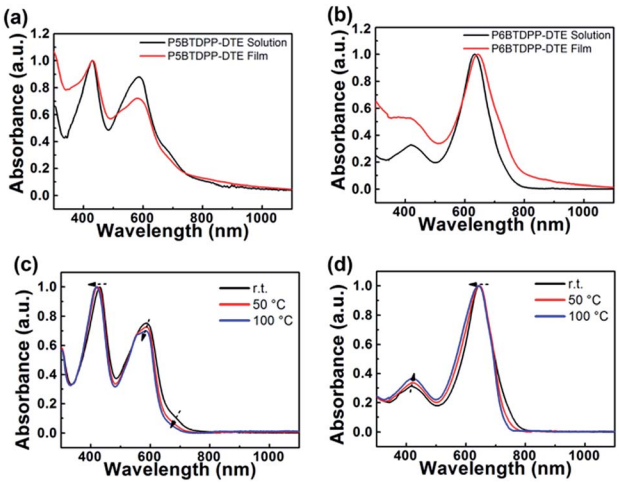

Fig. 3 UV-vis-NIR absorption spectra and *in situ* temperature-controlled absorption spectra (in dilute *o*-DCB) of P_5BTDPP-DTE (a and c) and P6BTDPP (b and d).

also indicated by the optical properties of the **5BrBTDPP** and **6BrBTDPP** monomers (Fig. S1†). As both monomers share D–A–D triad type electronic structures, the spectral shapes are akin to each other. Compared with **5BrBTDPP** monomer, **6BrBTDPP** shows a red-shifted absorption maximum of 582 nm, demonstrating that the electrons from 6-substituted bromine atoms are conjugated into the aromatic rings. Furthermore, both polymers exhibit inconspicuous signs of vibronic fine structures in the absorption spectra of dilute solution, closely resembling those of the solid-state films. The absence of obvious vibronic structure is attributed to weak π-ordering of the framework stemming from nonplanar energy-minima of optimized structures.[47] Slight bathochromic shift are observed in the films, indicative of moderate interchain interactions and backbone planarization. To confirm that the weak non-Gaussian shoulder peaks at *ca.* 750 nm are signs of aggregates, temperature-dependent absorption spectra were recorded in hot chlorobenzene (Fig. 3c and d). Heating the solution blueshifted the absorption and made the shoulder peaks disappearing, indicating the dispersal of aggregates and increased thermal motion of the polymer strands. As suggested by molecular modelling, the twist between benzothiophene and thiophene rings in PBTDPP backbones results in a loss of planarization and conjugation, therefore leading to a pronounced change in aggregation and absorption maximum compared with well-investigated thiophene-flanked DPP polymers.[25,48] For example, previously reported thiophene-flanked DPP containing analogue PDVT-10 shows an absorption maximum at *ca.* 800 nm in the solid film owing to the highly coplanar molecular conformations,[48] whereas the absorption maximum of less planar benzene-flanked DPP containing polymer C12DPP-π-BT is *ca.* 580 nm.[49] **P_6BTDPP-DTE** exhibits similar optical properties compared with the latter one because of the presence of dihedral torsions.

The frontier molecular orbital (FMO) energies of polymer films were investigated using cyclic voltammetry (CV) under

 This journal is © The Royal Society of Chemistry 2016

Published on 29 August 2016. Downloaded by Synchrotron Radiation Library on 11/09/2017 04:24:32.

a standard three-electrode cell electrochemical workstation (Fig. S2†). Onsets of both oxidation and reduction peaks and corresponding energy levels are listed in Table S1.† HOMO energy levels were calculated from the oxidation potential onset, yielding values of −4.90 and −4.88 eV for **P$_5$BTDPP-DTE** and **P$_6$BTDPP-DTE**, respectively, with an energy gap of around 1.5 eV. The relatively high HOMO energy levels arise from the stronger electron donating nature of benzothiophene compared with thienyl DPP analogues (*ca.* −5.3 eV).[48] The cross-conjugated polymer exhibits a slightly deeper HOMO energy level as expected, which can be ascribed to the fact that broken conjugation limits the electronic properties within one repeating unit. It should be noted that the presence of intense oxidation peaks suggest both polymers could operate as typical p-type materials, in agreement with the following discussed field-effect characteristics.

FET device performance

FET devices were fabricated to investigate the charge transport behaviours. All devices exhibited typical p-channel FET characteristics with bottom-gate-bottom-contact (BGBC) configurations using spin-coating technique on octadecyltrichlorosilane-treated Si/SiO_2 (300 nm) substrates. Detailed experimental conditions are concluded in ESI (Table S2†). In Fig. 4, typical p-type behaviour, good drain current saturation, and high on/off current ratios could be observed. Channel lengths of the devices were optimized to afford the highest carrier mobilities. The hole mobilities and on/off current ratios are summarized in Table 1, where the average values are obtained from twenty devices for each condition. **P$_6$BTDPP-DTE** shows a maximum mobility of 0.80 $cm^2\ V^{-1}\ s^{-1}$ with an average value of 0.43 $cm^2\ V^{-1}\ s^{-1}$, whereas the 5-bonded analogue **P$_5$BTDPP-DTE** exhibits a mobility of about 10^{-2} $cm^2\ V^{-1}\ s^{-1}$ (Fig. S3 and S4†), which is one order of magnitude lower. High-performance polymeric semiconductors usually exhibit non-ideal field-effect characteristics.[50,51] To avoid mobility overestimation, gate voltage dependence of charge carrier mobility is also presented in Fig. S5.† The differential mobility values extracted from high saturation regions exhibit a 2 to 3-fold decrease for both polymers. Although there are deviations from the ideal electrical characteristics, the carrier mobility comparison of the two polymers is still reliable because the difference in values is relatively large. As indicated by the differences of calculated FMO distributions, the cross-conjugated **P$_5$BTDPP-DTE** shows localized electronic structure, which hinders the intrachain transport. The results confirm the intrachain over interchain contribution of charge transport, and demonstrate that cross-conjugation in polymeric semiconductors is not in favour of obtaining high carrier mobility.

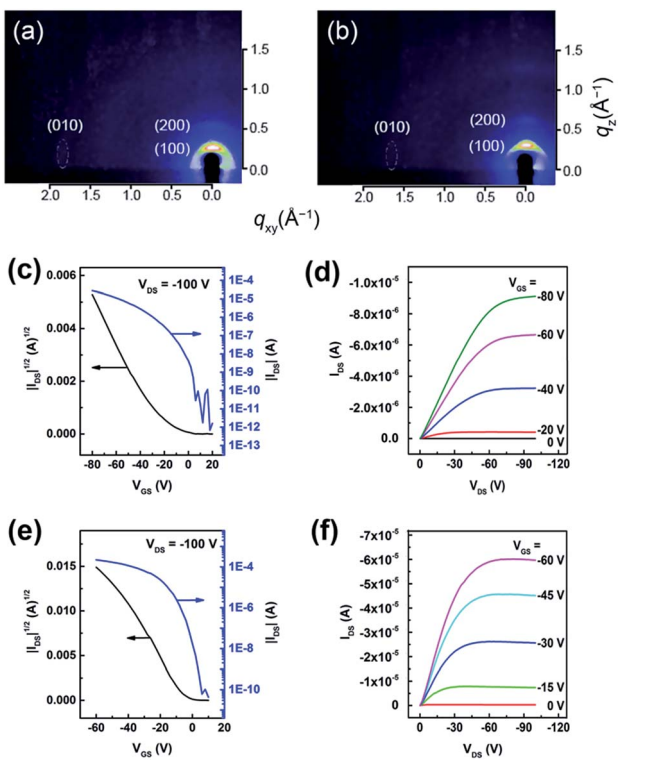

Fig. 4 GIXRD patterns of (a) P$_5$BTDPP-DTE and (b) P$_6$BTDPP-DTE. Transfer (c and e) and output characteristics (d and f) of typical FET devices based on P$_5$BTDPP-DTE (c and d) or P$_6$BTDPP-DTE (e and f).

Crystallinity and morphology

We employed gracing-incidence X-ray diffraction (GIXRD) and tapping-mode atomic force microscopy (AFM) to further study the crystallinity and morphology of PBTDPP thin films. In Fig. 4, both polymers show lamellar packing as is evident from the existence of moderate (*h*00) Bragg diffraction peaks in the out-of-plane direction and (010) peak in the in-plane direction. Calculated *d*–*d* spacing and π–π distances show distinct differences between the two polymers. For the annealed thin film of **P$_5$BTDPP-DTE**, up to second-order diffraction peak with a spacing of 22.1 Å was observed in the out-of-plane direction, indicating the edge-on orientation. Slight face-on orientations are also observed as evident from the (*h*00) diffraction peaks along the in-plane direction (Fig. S6 and S7†). A short *d*–*d* spacing of 19.2 Å is obtained for **P$_6$BTDPP-DTE**, suggesting the alkyl chain orientation is slightly less perpendicular to the polymer backbone than the 5-bonded analogue. This result is reasonable, as is in close agreement with the calculated structures of optimized trimmers. According to the previously reported π–π stacking assisted hopping mechanism, a short π–π stacking distance may facilitate better charge transport.[25]

Table 1 FET characteristics and GIXRD properties of PBTDPP-DTE based thin film transistors

Polymer	Channel length (μm)	Mobility[a] ($cm^2\ V^{-1}\ s^{-1}$)	I_{on}/I_{off}	π–π (Å)	*d*–*d* (Å)
P$_5$BTDPP-DTE	20	1.58×10^{-2} (7.16×10^{-3})	10^5 to 10^7	3.44	22.1
P$_6$BTDPP-DTE	50	0.80 (0.43)	10^5 to 10^7	3.75	19.2

[a] Maximum values of hole mobility, values in parentheses are average values.

Published on 29 August 2016. Downloaded by Synchrotron Radiation Library on 11/09/2017 04:24:32.

Nevertheless, **P_5BTDPP-DTE** thin film exhibits a π–π stacking of 3.44 Å, much shorter than that of **P_6BTDPP-DTE** thin film (3.75 Å). The shorter π–π stacking of cross-conjugated polymer may be ascribed to the electrostatic and dispersion interactions stemming from the more localized overlaps of frontier molecular π-orbitals. We deduce that charge hopping along the π–π stacking is less contributing to mobilities than the effective conjugation, indicating that the intramolecular transport may play the dominant role for semiconducting polymers. The comparison of π–π stacking distance is only meaningful for identical polymer backbones, because the identical backbone generally packs similarly that the interchain charge hopping ability could be a function of the π–π stacwking distance. This conclusion is consistent with the charge transporting mechanism put forward by Mei *et al.* using conjugation-break spacers in semiconducting polymers.[52,53] AFM images were obtained under different annealing temperatures (Fig. S8†). The intertwined grain-like structures are observed in the height AFM images of **P_5BTDPP-DTE** and **P_6BTDPP-DTE** thin films. With the increase of annealing temperature, the AFM images of these polymer films show crystalline tendency and larger root-mean-square (RMS) deviations, indicating that the polymers tend to form larger grains to facilitate charge transport.[48,54,55]

Conclusions

In summary, we have developed new benzothiophene-flanked DPP copolymers and investigated their FET characteristics. Two isomeric polymers show different electronic properties and crystalline behaviours. The linearly-conjugated **P_6BTDPP-DTE** shows much higher mobilities (0.80 $cm^2 V^{-1} s^{-1}$) than the cross-conjugated **P_5BTDPP-DTE** (1.58×10^{-2} $cm^2 V^{-1} s^{-1}$), suggesting that the intrachain transport plays a more important role in charge transport for polymeric semiconductors.

Acknowledgements

This work was financially supported by the National Natural Science Foundation of China (21474116 and 51233006) and the Strategic Priority Research Program of the Chinese Academy of Sciences (XDB12030100). The GIXRD results were tested at the BL16B1 Station of Shanghai Synchrotron Radiation Facility (SSRF), 23A1 Station of National Synchrotron Radiation Research Center (NSRRC, Taiwan), and 1W1A Station of Beijing Synchrotron Radiation Facility. The authors gratefully acknowledge the assistance during the experiments.

Notes and references

1 M. Nakano, I. Osaka and K. Takimiya, *Macromolecules*, 2015, **48**, 576.
2 L. Wang, X. Xie, S. Shi, K. Shi, Z. Mao, W. Zhang, H. Wang and G. Yu, *Polymer*, 2015, **68**, 302.
3 R. S. Ashraf, I. Meager, M. Nikolka, M. Kirkus, M. Planells, B. C. Schroeder, S. Holliday, M. Hurhangee, C. B. Nielsen, H. Sirringhaus and I. McCulloch, *J. Am. Chem. Soc.*, 2015, **137**, 1314.
4 J. Y. Back, H. Yu, I. Song, I. Kang, H. Ahn, T. J. Shin, S.-K. Kwon, J. H. Oh and Y.-H. Kim, *Chem. Mater.*, 2015, **27**, 1732.
5 B. Wang, J. Zhang, H. L. Tam, B. Wu, W. Zhang, M. S. Chan, F. Pan, G. Yu, F. Zhu and M. S. Wong, *Polym. Chem.*, 2014, **5**, 836.
6 X. Guo, A. Facchetti and T. J. Marks, *Chem. Rev.*, 2014, **114**, 8943.
7 Z. Fei, P. Pattanasattayavong, Y. Han, B. C. Schroeder, F. Yan, R. J. Kline, T. D. Anthopoulos and M. Heeney, *J. Am. Chem. Soc.*, 2014, **136**, 15154.
8 X. Guo, J. Quinn, Z. Chen, H. Usta, Y. Zheng, Y. Xia, J. W. Hennek, R. P. Ortiz, T. J. Marks and A. Facchetti, *J. Am. Chem. Soc.*, 2013, **135**, 1986.
9 R. Noriega, J. Rivnay, K. Vandewal, F. P. V. Koch, N. Stingelin, P. Smith, M. F. Toney and A. Salleo, *Nat. Mater.*, 2013, **12**, 1037.
10 Y. He, C. Guo, B. Sun, J. Quinn and Y. Li, *Chem. Commun.*, 2015, **51**, 8093.
11 K. H. Park, K. H. Cheon, Y. J. Lee, D. S. Chung, S. K. Kwon and Y. H. Kim, *Chem. Commun.*, 2015, **51**, 8120.
12 H. Hu, J. He, H. Zhuang, E. Shi, H. Li, N. Li, D. Chen, Q. Xu, J. Lu and L. Wang, *J. Mater. Chem. C*, 2015, **3**, 8605.
13 J. Shin, G. E. Park, D. H. Lee, H. A. Um, T. W. Lee, M. J. Cho and D. H. Choi, *ACS Appl. Mater. Interfaces*, 2015, **7**, 3280.
14 B. He, B. A. Zhang, F. Liu, A. Navarro, M. P. Fernández-Liencres, R. Lu, K. Lo, T. L. Chen, T. P. Russell and Y. Liu, *ACS Appl. Mater. Interfaces*, 2015, **7**, 20034.
15 B. He, A. B. Pun, L. M. Klivansky, A. M. McGough, Y. Ye, J. Zhu, J. Guo, S. J. Teat and Y. Liu, *Chem. Mater.*, 2014, **26**, 3920.
16 B. He, A. B. Pun, D. Zherebetskyy, Y. Liu, F. Liu, L. M. Klivansky, A. M. McGough, B. A. Zhang, K. Lo, T. P. Russell, L. Wang and Y. Liu, *J. Am. Chem. Soc.*, 2014, **136**, 15093.
17 D. Gao, K. Tian, W. Zhang, J. Huang, Z. Chen, Z. Mao and G. Yu, *Polym. Chem.*, 2016, **7**, 4046.
18 Y. He, C. Guo, B. Sun, J. Quinn and Y. Li, *Polym. Chem.*, 2015, **6**, 6689.
19 C. Li, N. Zheng, H. Chen, J. Huang, Z. Mao, L. Zheng, C. Weng, S. Tan and G. Yu, *Polym. Chem.*, 2015, **6**, 5393.
20 D. I. James, S. Wang, W. Ma, S. Hedström, X. Meng, P. Persson, S. Fabiano, X. Crispin, M. R. Andersson, M. Berggren and E. Wang, *Adv. Electron. Mater.*, 2016, **2**, 1500313.
21 G. Zhang, J. Guo, M. Zhu, P. Li, H. Lu, K. Cho and L. Qiu, *Polym. Chem.*, 2015, **6**, 2531.
22 J. D. Yuen and F. Wudl, *Energy Environ. Sci.*, 2013, **6**, 392.
23 J. Li, Y. Zhao, H. S. Tan, Y. Guo, C.-A. Di, G. Yu, Y. Liu, M. Lin, S. H. Lim, Y. Zhou, H. Su and B. S. Ong, *Sci. Rep.*, 2012, **2**, 754.
24 S. E. Wheeler, *J. Am. Chem. Soc.*, 2011, **133**, 10262.
25 Y. Li, P. Sonar, S. P. Singh, M. S. Soh, M. van Meurs and J. Tan, *J. Am. Chem. Soc.*, 2011, **133**, 2198.
26 P. Sonar, S. P. Singh, Y. Li, M. S. Soh and A. Dodabalapur, *Adv. Mater.*, 2010, **22**, 5409.
27 T. Lei, J.-H. Dou and J. Pei, *Adv. Mater.*, 2012, **24**, 6457.

 This journal is © The Royal Society of Chemistry 2016

Published on 29 August 2016. Downloaded by Synchrotron Radiation Library on 11/09/2017 04:24:32.

28 I. Kang, H.-J. Yun, D. S. Chung, S.-K. Kwon and Y.-H. Kim, *J. Am. Chem. Soc.*, 2013, **135**, 14896.
29 H. Bronstein, Z. Chen, R. S. Ashraf, W. Zhang, J. Du, J. R. Durrant, P. Shakya Tuladhar, K. Song, S. E. Watkins, Y. Geerts, M. M. Wienk, R. A. J. Janssen, T. Anthopoulos, H. Sirringhaus, M. Heeney and I. McCulloch, *J. Am. Chem. Soc.*, 2011, **133**, 3272.
30 I. Meager, R. S. Ashraf, S. Rossbauer, H. Bronstein, J. E. Donaghey, J. Marshall, B. C. Schroeder, M. Heeney, T. D. Anthopoulos and I. McCulloch, *Macromolecules*, 2013, **46**, 5961.
31 K. Takimiya, H. Ebata, K. Sakamoto, T. Izawa, T. Otsubo and Y. Kunugi, *J. Am. Chem. Soc.*, 2006, **128**, 12604.
32 H. Ebata, T. Izawa, E. Miyazaki, K. Takimiya, M. Ikeda, H. Kuwabara and T. Yui, *J. Am. Chem. Soc.*, 2007, **129**, 15732.
33 H. Dong, H. Zhu, Q. Meng, X. Gong and W. Hu, *Chem. Soc. Rev.*, 2012, **41**, 1754.
34 M. Gholami and R. R. Tykwinski, *Chem. Rev.*, 2006, **106**, 4997.
35 M. Murai, S.-Y. Ku, N. D. Treat, M. J. Robb, M. L. Chabinyc and C. J. Hawker, *Chem. Sci.*, 2014, **5**, 3753.
36 I. Osaka, T. Abe, S. Shinamura and K. Takimiya, *J. Am. Chem. Soc.*, 2011, **133**, 6852.
37 J. Yao, Z. Cai, Z. Liu, C. Yu, H. Luo, Y. Yang, S. Yang, G. Zhang and D. Zhang, *Macromolecules*, 2015, **48**, 2039.
38 Z. Zhao, F. Zhang, X. Zhang, X. Yang, H. Li, X. Gao, C.-a. Di and D. Zhu, *Macromolecules*, 2013, **46**, 7705.
39 I. Osaka, Y. Houchin, M. Yamashita, T. Kakara, N. Takemura, T. Koganezawa and K. Takimiya, *Macromolecules*, 2014, **47**, 3502.
40 S.-W. Cheng, D.-Y. Chiou, C.-E. Tsai, W.-W. Liang, Y.-Y. Lai, J.-Y. Hsu, C.-S. Hsu, I. Osaka, K. Takimiya and Y.-J. Cheng, *Adv. Funct. Mater.*, 2015, **25**, 6131.
41 G. W. P. van Pruissen, J. Brebels, K. H. Hendriks, M. M. Wienk and R. A. J. Janssen, *Macromolecules*, 2015, **48**, 2435.
42 S. Pluczyk, W. Kuznik, M. Lapkowski, R. R. Reghu and J. V. Grazulevicius, *Electrochim. Acta*, 2014, **135**, 487.
43 K. Miyagi, K. Moriyama and H. Togo, *Eur. J. Org. Chem.*, 2013, **2013**, 5886.
44 S. Talukdar, J.-L. Hsu, T.-C. Chou and J.-M. Fang, *Tetrahedron Lett.*, 2001, **42**, 1103.
45 K. C. Lee, G.-S. Ryu, S. Chen, G. Kim, Y.-Y. Noh and C. Yang, *Org. Electron.*, 2016, **37**, 402.
46 T. Lei, J.-H. Dou, X.-Y. Cao, J.-Y. Wang and J. Pei, *J. Am. Chem. Soc.*, 2013, **135**, 12168.
47 N. E. Jackson, K. L. Kohlstedt, B. M. Savoie, M. Olvera de la Cruz, G. C. Schatz, L. X. Chen and M. A. Ratner, *J. Am. Chem. Soc.*, 2015, **137**, 6254.
48 H. Chen, Y. Guo, G. Yu, Y. Zhao, J. Zhang, D. Gao, H. Liu and Y. Liu, *Adv. Mater.*, 2012, **24**, 4618.
49 W. Li, T. Lee, S. J. Oh and C. R. Kagan, *ACS Appl. Mater. Interfaces*, 2011, **3**, 3874.
50 H. Sirringhaus, *Adv. Mater.*, 2014, **26**, 1319.
51 E. G. Bittle, J. I. Basham, T. N. Jackson, O. D. Jurchescu and D. J. Gundlach, *Nat. Commun.*, 2016, **7**, 10908.
52 Y. Zhao, X. Zhao, Y. Zang, C.-a. Di, Y. Diao and J. Mei, *Macromolecules*, 2015, **48**, 2048.
53 Y. Zhao, X. Zhao, M. Roders, G. Qu, Y. Diao, A. L. Ayzner and J. Mei, *Chem. Mater.*, 2015, **27**, 7164.
54 H. Chen, Y. Guo, Z. Mao, G. Yu, J. Huang, Y. Zhao and Y. Liu, *Chem. Mater.*, 2013, **25**, 3589.
55 T. Lei, Y. Cao, X. Zhou, Y. Peng, J. Bian and J. Pei, *Chem. Mater.*, 2012, **24**, 1762.